IEEE Access
Multidisciplinary | Rapid Review | Open Access Journal

Received March 20, 2020, accepted April 1, 2020, date of publication April 23, 2020, date of current version May 7, 2020.

Digital Object Identifier 10.1109/ACCESS.2020.2989678

Ultra-Wide and Flattened Optical Frequency Comb Generation Based on Cascaded Phase Modulator and LiNbO3-MZM Offering Terahertz Bandwidth

SIBGHAT ULLAH[1,3], RAHAT ULLAH[2], QI ZHANG[1,3], HAFIZ AHMAD KHALID[1,3], KAMRAN ALI MEMON[1,3], (Member, IEEE), ADIL KHAN[3], FENG TIAN[1,3], AND XIN XIANGJUN[1,3]

[1]State Key Laboratory of Information Photonics and Optical Communications, Beijing University of Posts and Telecommunications, Beijing 100876, China
[2]Institute of Opto-Electronics, Nanjing University of Information Science and Technology, Nanjing 210044, China
[3]School of Electronics Engineering, Beijing University of Posts and Telecommunications, Beijing 100876, China

Corresponding author: Rahat Ullah (r.rahatullah@gmail.com)

This work was supported in part by the Natural National Science Foundation of China (NSFC) under Grant 61727817, Grant 61605013, Grant 61875248, Grant 61672290, and Grant 61675030, and in part by the Fund of State Key Laboratory of IPOC (BUPT).

ABSTRACT In this paper, a new technique for generation of ultra-wide and flattened optical frequency comb (OFC) based on serial cascading of a phase modulator and dual-driven Lithium-Niobate Mach Zehnder modulator (DD-$LiNbO_3$-MZM) is proposed. Over 60 carriers were generated by carefully adjusting the RF switching voltage (RFSV) of the DD-$LiNbO_3$-MZM and the signal frequency of the sinusoidal wave (RF) source. A low power amplified RF source with a signal driving power of 16.9dBm is applied, and the power of CW laser is kept at 3dBm. The frequency spacing (FS) is kept at 20GHz for generating the maximum number of carriers. Nonetheless, the scheme is also tested for the FSs of 64GHz, and 32GHz. Each scenario is examined in simulation environment and the main outcomes are highlighted. The proposed scheme is comparatively simple and the FS varies with the applied RF source on the modulators. The achieved OFC lines have a tone-to-noise ratio (TNR) of over 45dB with an undesired side mode suppression ratio of approximately 20dB. The comb lines are almost flat with a varying power deviation of around 0dB-6dB which is optimized to nearly 0.12dB. Furthermore, the impact of the RFSV on the generated number of carriers is studied in detail. The scheme is analyzed in terms of cost efficiency, power deviations, TNR, optical signal to noise ratio, and number of achieved comb lines.

INDEX TERMS Optical frequency comb, intensity modulation, Mach-Zehnder modulator, phase modulator.

I. INTRODUCTION

Optical frequency comb (OFC) generation have attracted many researchers due to its diverse characteristics of transmitting higher data rates at lower cost. It has been widely used as a multi wavelength source at the OLT side of an optical communication system in optical orthogonal frequency division multiplexing, optical time division multiplexing, quadrature amplitude modulation, and dense wavelength division multiplexing [1]–[8]. It has been a hotspot for researchers due to its importance and applications in the area of optical communications, optical arbitrary waveform generation, and optical frequency meteorology [9]–[12]. The generated OFC is required to have great flatness, high tone to noise ratio (TNR), variable frequency spacing, and may effectively reduce the optical line terminal (OLT) cost by replacing multiple laser sources and various other components.

In recent years, various methods and configurations are proposed for OFC generation [13]–[28]. The most common configurations used for generating OFC lines are: mode-locked lasers (MLL), recirculating frequency shifting (RFS) loop, and nonlinear effects in a highly nonlinear medium [13]–[18]. The first method is based on MLL; the generated OFCs have a high bandwidth but it is not easy to

The associate editor coordinating the review of this manuscript and approving it for publication was Qunbi Zhuge.

control and adjust the OFC generator. The second method is based on RFS loop; variety of research articles have reported that RFS loop can obtain more comb lines, however, the structure of the RFS loop is complex and requires more components. For example, in ref [16], the dual RFS loop follows a complex structure, the generated comb lines are not stable, and it is hard to maintain. In the generated spectra, a maximum power deviation of over 10dB can be seen among the comb lines. The last method is based on the non-linear effects in highly non-linear medium; the generated OFC suffers from flatness of the comb lines and lacks continuous tunability of the generated spectra.

Generation of OFC using optical modulation is another interesting technique and has already been widely studied. This technique can be explained in two parts: (i) the first one is based on the utilization of either intensity modulators (IMs) [19], [20], cascaded or parallel IMs [1], [21]–[23], phase modulators (PMs) [24]–[26], or polarization modulators [27]. (ii) the second one is based on the hybrid utilization of different modulators such as cascaded configuration of PM and IMs [28]. This method is widely and most commonly used to generate OFC lines due to its simple and cost-efficient structure. However, sometimes, it requires high driving voltage of the RF source [29].

Among all these methods, the most commonly used method for OFC generation is the use of IMs due to its flexibility and high quality. The IMs are mostly driven by a light source and a radio frequency (RF) source. The driving signal frequency of the RF source are mostly tunable and can be adjusted to obtain an ultra-flat OFC spectra.

In the proposed scheme, serially cascaded optical phase modulator (PM) and dual-driven Lithium-Niobate Mach Zehnder modulator (DD-$LiNbO_3$-MZM) is utilized for the generation of OFC. An amplified sine wave with a signal driving power of 16.9dBm is used as a low driving RF source. A CW laser having frequency 193.1THz and 3dBm power is utilized to generate the light-wave signal. The RF source is divided in three discrete parts by utilizing a 1×3 fork whereby the frequency and signal power is not affected and the same signal is applied across each sub-part. The electrical input arm of the PM is driven by the RF source and the optical input arm is injected by the CW laser. Whereas, the optical input arm of the DD-$LiNbO_3$-MZM is driven by the generated output of the PM and both electrical input arms of the DD-$LiNbO_3$-MZM are driven by the low powered RF source having same power and frequency. Here, the PM converts the signal into a wideband signal which consists of ultra-short pulses and is further widened by utilizing the DD-$LiNbO_3$-MZM. The output spectra of the PM consist of limited and unstable carriers which is then injected into the optical input port of the DD-$LiNbO_3$-MZM. The DD-$LiNbO_3$-MZM normalizes the electrical signal with the help of biasing voltage of 0V and -2V, and modulation voltage of 4V and -4V. At this stage, an unstable optical spectrum is achieved. However, the RF switching voltage (RFSV) plays an important role in the stability of the generated carriers. After carefully observing the performance of the scheme under various conditions, an almost flattened optical spectra of 63 carriers, having a frequency spacing (FS) of 20GHz, is achieved with a maximum power deviation (PD) of around $\sim$6dB among the left-most and right-most 7carriers. The PD is reduced to a maximum of 0.12dB by optimizing the results with an optical filter. The TNR is above 45dB with an undesired side mode suppression ratio (USMSR) of around 20dB. The scheme is also tested for stability under various frequencies of the RF source and it is observed that the scheme can produce even more stable results for higher FSs. The performance of the proposed scheme is analyzed in terms of cost efficiency, number of generated carriers, their PDs, tone to noise ratios (TNRs), and the effect of the RFSV of the DD-$LiNbO_3$-MZM is studied.

The main contributions of this article are summarized as follows:

- A new OFC generation technique based on cascaded phase and DD-$LiNbO_3$-MZM is proposed.
- An amplified RF source with low driving voltage is utilized.
- Theoretical analysis and simulation have been carried out to validate the results and claims.
- The generated results are optimized with the help of an optical filter to reduce the PD among the comb lines.
- The bandwidth of the OFC spectra is enhanced, cost is reduced, whereas number of comb lines are increased compared to most of the schemes.

Recently, we proposed two techniques for OFC generation based on a single IM [29], [30]. The deployment of the schemes was discussed in details. In contrast to the proposed scheme, the two schemes utilized a single drive MZM with a higher RF driving voltage, however, cascaded configuration of PM and $LiNbO_3$-MZM is utilized in the current scheme. The number of generated comb lines is greatly enhanced and a higher bandwidth is achieved.

The rest of the paper is structured as follows: section one contains the introduction part where a study of several articles is presented along with our previous contributions to the concerned topic. The second section covers the principle of operation of the proposed OFC scheme. The schematics and structure of the proposed scheme is discussed in details. The simulation findings are demonstrated and discussed in the third section. At the end, the paper is concluded with a comprehensive conclusion.

II. PRINCIPLE OF OPERATION

In the proposed scheme, a centrally flattened OFC spectra is achieved by utilizing a PM and DD-$LiNbO_3$-MZM in cascading mode. The scheme also utilizes an amplified RF source and a CW laser. The RF source has a signal driving power of 16.9dBm and frequency of 20GHz. The RF source is split in three sub-parts with the help of a 1×3 fork which does not affect the frequency, phase or the driving voltage of the signal. The CW laser has a frequency of 193.1THz and

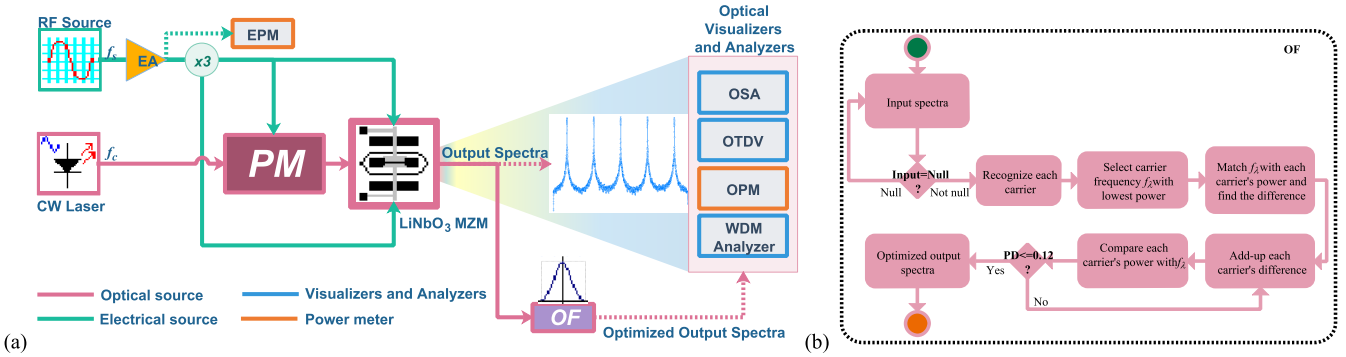

FIGURE 1. (a) Schematic diagram of the proposed OFC scheme. (b) working mechanism of the OF. [RF; radio frequency, CW; continuous wave, EA; electrical amplifier, EPM; electrical power meter, OSA; optical spectrum analyzer, OTDV; optical time domain visualizer, OPM; optical power meter, OF; optical filter, PD; power deviation/difference].

3dBm power with a linewidth of 10MHz. The PM is used to impose a phase modulation on the optical signal via electrical modulation. The PM has an optical and electrical input arm where a CW laser is used to inject a light wave signal into the optical input arm, whereby, the electrical input arm is driven by the RF source. The output of the light source can be expressed as

$$E_c = E_o e^{j2\pi f_c t} \tag{1}$$

and output of the RF source can be written as

$$Y_{rf}(t) = m.\sin(2\pi f_s t + \phi) \tag{2}$$

where f_s represents the number of oscillations per second, m represents the amplitude of the signal, $2\pi f_s$ represents the angular frequency and ϕ represents the initial phase of the electrical signal. The output of the PM can be expressed as

$$E_{pmout} = E_{in}.e^{j.\Delta\phi.Y_{rf}(t)} \tag{3}$$

where E_{pmout} is the output optical signal of the PM, $Y_{rf}(t)$ is the input electrical signal, $\Delta\phi$ represents the phase shift induced by the modulator, and E_{in} is the input optical signal. By injecting both RF and CW source at the input electrical and input optical arm of the PM, the output of the PM can be given as [26], [31]

$$\begin{aligned} E_{pmout} &= E_c.e^{j.\Delta\varphi.Y_{rf}(t)} \\ &= E_o e^{(j2\pi f_c t)}.e^{(j.\Delta\varphi.m.\sin(2\pi f_s t+\phi))} \end{aligned} \tag{4}$$

Expanding the above equation with Jacobi Anger expansion, we get [26], [31]

$$E_{pmout} = E_c \sum_{n=-\infty}^{n=+\infty} J_n(\pi.m).\exp(\mathrm{j}2\pi(\mathrm{f_c} + \mathrm{nf_s})\mathrm{t}) \tag{5}$$

where m is the modulation index of the modulator and $J_n(\pi.m)$ represents the first kind of Bessel function of order "n". Equation 5 represents the generated output spectra of the PM with frequency ($\mathrm{f_c}+\mathrm{nf_s}$) where $\mathrm{n} = \pm1, \pm2, \ldots, \pm\mathrm{n}$. The input RF signal is normalized between 0 and 1.

Next to the PM, a DD-$LiNbO_3$-MZM is utilized to perform intensity modulation on the output spectra generated by the PM and tune the power variations of even and odd sidebands at the same level to obtain a flattened optical spectrum at the output. The schematic diagram of the proposed scheme can be seen in Figure 1 (a).

The operational principles of MZMs are based on the electro-optic effect. This effect is characterized by the variation in the applied electric field which causes variance of the refractive index in the modulator arms. The input optical signal is divided in two equivalent parts; lower arm and upper arm of the modulator. The modulator is driven by an RF source and different transmission speeds can be achieved based on the driving voltage of the input electrical signal. The DD-$LiNbO_3$-MZM has an optical input arm and two electrical input arms. The optical input arm is injected by the output of the PM, whereby, the electrical input arms are driven by the RF source with frequency variation of 2^{n+1} where n = 4, and 5. The extinction ratio of the DD-$LiNbO_3$-MZM is kept at 20dB, a DC bias voltage of 4v to turn the device on or off, and the RFSV varies from 0.2V to 4V with an insertion loss of 5dB (for graphical illustrations of OSNR, and total noise power calculation, the lowest value of −4V is also considered). The impact of the RFSV on the generated optical spectra is studied and further discussed in the coming sections. The DD-$LiNbO_3$-MZM normalizes the input electrical signals between −0.5 and 0.5 at both input arms which is then multiplied by modulation voltage 1 (which in this case is kept at 4V) and modulation voltage 2 (which is kept at −4V). This can be expressed as

$$V_1(t) = NES * MV_1 \tag{6}$$

$$V_2(t) = NES * MV_2 \tag{7}$$

where NES represents the normalized electrical signal, MV_1 represents the modulation voltage 1, and MV_2 represents the modulation voltage 2. $E_{in}(t)$ represents the optical input signal at the input optical arm of the DD-$LiNbO_3$-MZM, $v_1(t)$, $v_2(t)$ represents the electrical input signals at the electrical input arm1, 2, respectively, and $E_{out}(t)$ represents the output optical spectra at the optical output arm of the DD-$LiNbO_3$-MZM. The output of the DD-$LiNbO_3$-MZM

can be expressed as

$$E_{out}(t) = \frac{E_{in}(t)\, V_{\pi DC}(t)}{10(I_{loss}/20)} \cdot \left[\begin{array}{l} SR \cdot e^{(j\pi v_2(t)/V_{\pi RF} + j\pi v_{bias2}/V_{\pi DC})} \\ +(1-SR) \cdot e^{(j\pi v_1(t)/V_{\pi RF} + j\pi v_{bias1}/V_{\pi DC})} \end{array} \right] \quad (8)$$

where $E_{out}(t)$ represents the output optical signal, $E_{in}(t)$ denotes the input optical signal which in this case is the output optical spectra of the PM, insertion loss is represented by I_{loss} which in this case is kept at 5dB, $v_1(t)$ and $v_2(t)$ represents the electrical voltages for upper and lower arms of the modulator. The value of $v_1(t)$ is kept at 4V and value of $v_2(t)$ is kept at -4V. $v_{bias1}(t)$ and $v_{bias2}(t)$ represents the bias voltage 1 and bias voltage 2. The RFSV is represented by $V_{\pi RF}$, and the DC bias voltage is represented by $V_{\pi DC}$. The power splitting ratio of both Y-branch waveguides is represented by SR which can be further expressed as

$$SR = \left(1 - \frac{1}{\sqrt{\varepsilon_r}}\right)/2 \quad \varepsilon_r = 10^{E_r/10} \quad (9)$$

where the E_r is defined by the parametric value of Extinction ratio. By substituting the value of the insertion loss and SR in equation 8, we can get

$$E_{out}(t) = \frac{E_{in}(t)\, V_{\pi DC}(t)}{2.5} \cdot \left[\begin{array}{l} \left(1 - \frac{1}{\sqrt{10^{E_r/10}}}\right) \cdot e^{(j\pi v_2(t)/V_{\pi RF} + j\pi v_{bias2}/V_{\pi DC})}/2 \\ +\left(1 - \left(1 - \frac{1}{\sqrt{10^{E_r/10}}}\right)/2\right) \cdot e^{(j\pi v_1(t)/V_{\pi RF} + j\pi v_{bias1}/V_{\pi DC})} \end{array} \right] \quad (10)$$

The above equation can be simplified as

$$E_{out}(t) = \frac{E_{in}(t)\, V_{\pi DC}(t)}{2.5} \cdot \left[\begin{array}{l} (0.45) \cdot e^{(j\pi v_2(t)/V_{\pi RF} + j\pi v_{bias2}/V_{\pi DC})} \\ +(0.55) \cdot e^{(j\pi v_1(t)/V_{\pi RF} + j\pi v_{bias1}/V_{\pi DC})} \end{array} \right] \quad (11)$$

The above equation represents the generated optical frequency comb at the output port of the DD-LiNbO$_3$-MZM. By carefully adjusting the bias and modulation voltage1, 2, and switching bias and RF voltages, an OFC spectra of ∼63 healthy carriers is achieved. The signal is measured and visualized with an optical spectrum analyzer (OSA), optical time domain visualizer (OTDV), optical power meter (OPM), and WDM analyzer as shown in Figure 1 (a). The PD among the centered carriers is about 0.01dB-1.5dB, however, the PD on the sidebands can reach up to a maximum of ∼6dB. This is the scenario for 20Ghz FS. To reduce the PDs and get an overall flattened OFC spectra, an optical filter is utilized to perform gain flattening and an optimized OFC is achieved where the PD is reduced to a maximum of ∼0.12dB. The total bandwidth supported by the scheme is around 1260GHz. The working mechanism of the optical filter is shown in Figure 1 (b). The simulations are carried out in Optisystem and the parametric values of DD-LiNbO$_3$-MZM and layout parameters are specified in Table 1.

TABLE 1. Simulation parameters.

Parameter Name	Value
Layout Parameters	
Sequence length	128bits
Samples per bit	64
Number of samples	8192
Simulation Window	
Bit rate/	20e+009 bits/s
Time window/	12.8e-009s
Sample rate	640e+009Hz
DD-LiNbO$_3$-MZM	
Extinction ratio	20dB
Switching bias voltage	4V
RFSV	0.2-0.4V
Insertion loss	5dB

III. SIMULATION RESULTS AND DISCUSSIONS

In order to confirm the likelihood and need of the proposed OFC generation scheme, theoretical and principle analysis were performed for the cascaded PM and DD-LiNbO$_3$-MZM. Here, the FS of 20GHz, 32GHz, and 64GHz were considered to examine the stability and scalability of the scheme under various FSs. In the first case, ∼63 stable and healthy carriers were generated by carefully adjusting the RFSV and biasing voltages of the DD-LiNbO$_3$-MZM. In the second case, the FS is increased to 32GHz and 41 stable and healthy carriers were generated with high TNR and an almost flattened spectra among the central carriers. In the third case, the FS is doubled (64GHz) and an overall OFC spectra of 21 stable and healthy carriers is achieved. The simulation results of these cases can be seen in Figure 2. Furthermore, the PD is reduced by performing gain flattening on the generated spectra of each event. At the output port of the DD-LiNbO$_3$-MZM, an optimized optical filter is used to further stabilize the generated spectra and reduce the PDs among the carriers. In the first instance, the PD is reduced to a maximum of ∼0.12dB, whereas, ∼0.08dB, and ∼0.07dB PDs are achieved for the rest of the instances. The optimized simulation results are shown in Figure 3.

Figure 2(a, b, and c) shows the simulated output spectra of the DD-LiNbO$_3$-MZM when the FS is kept at 20GHz, 32GHz, and 64GHz. It can be seen that the maximum number of carriers can be achieved when the lowest FS is considered. However, with increasing the FS, although the number of carriers is reduced, the stability of the scheme is enhanced. The graphical illustration of the PD of all the given cases is shown in Figure 4.

The spectral components (SCs) of the OFC spectra can be determined using equation 12.

$$SC = \sum_{i=1}^{n} f_c \pm i f_s \quad \therefore n = 32, 16, 8 \quad (12)$$

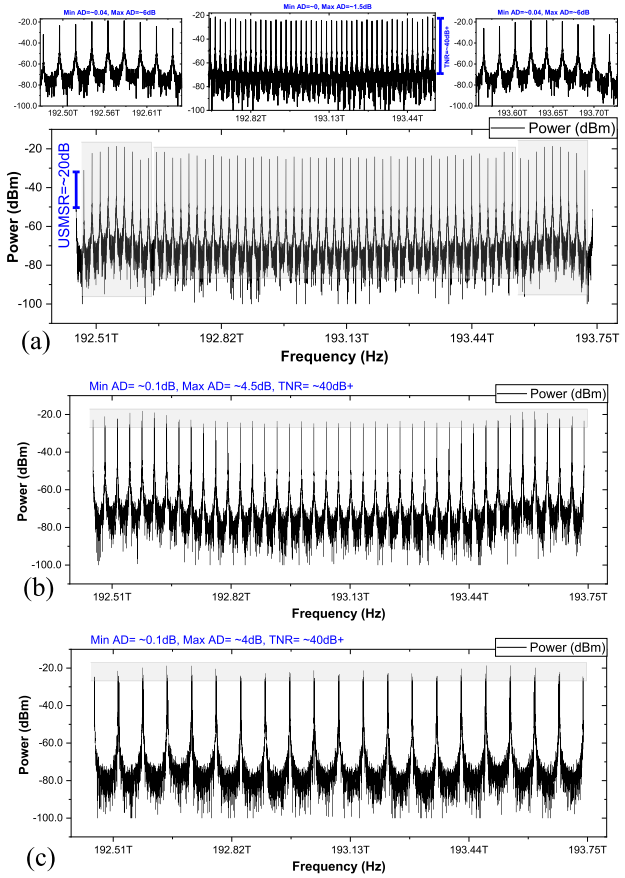

FIGURE 2. Simulation results of the proposed OFC scheme. (a) 20GHz, (b) 32GHz, and (c) 64GHz.

TABLE 2. Spectral components of the generated OFC spectra.

	Spectral Components
FS=20GHz	*fc, fc±fs, fc±2fs, fc±3fs, fc±4fs, fc±5fs, fc±6fs, fc=±7fs, fc±8fs, f=±9fs, fc±10fs, ..., fc±31fs*
FS=32GHz	*fc, fc±fs, fc±2fs, fc±3fs, fc±4fs, fc±5fs, fc±6fs, f=±7fs, fc±8fs, ..., fc±16fs*
FS=64GHz	*fc, fc±fs, fc±2fs, fc±3fs, fc±4fs, fc±5fs, fc±6fs, f=±7fs, fc±8fs*

Using the equation, the SCs of the generated OFC are listed in Table 2.

The graphs in Figure 4 shows minimum and maximum PDs among the carriers starting from central position and spreading towards left and right direction. The PDs of the OFC spectra prior to gain flattening is illustrated in Figure 4 (a, b, and c), and post optimization is shown in Figure 4(d). The filter transmission function is illustrated in Figure 4(e).

Figure 5(a, & b) shows the impact of the varying RFSV on the OSNR (dB) and total noise power (dBm) of the generated spectra. It can be seen that an OSNR of over 50dB is achieved along with a total noise power of approximately −75dBm, which imposes the effectiveness of the scheme. Moreover, the RFSV plays an important role in controlling the number of generated carriers and maintaining the PD among them. The impact of varying RFSV on the generated number of carriers can be seen in Figure 6.

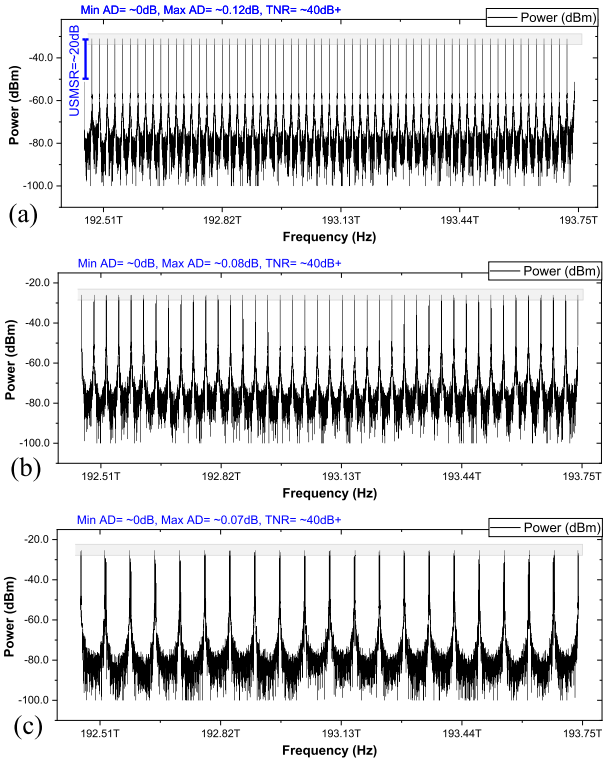

FIGURE 3. Simulated OFC spectra after performing filter optimization.

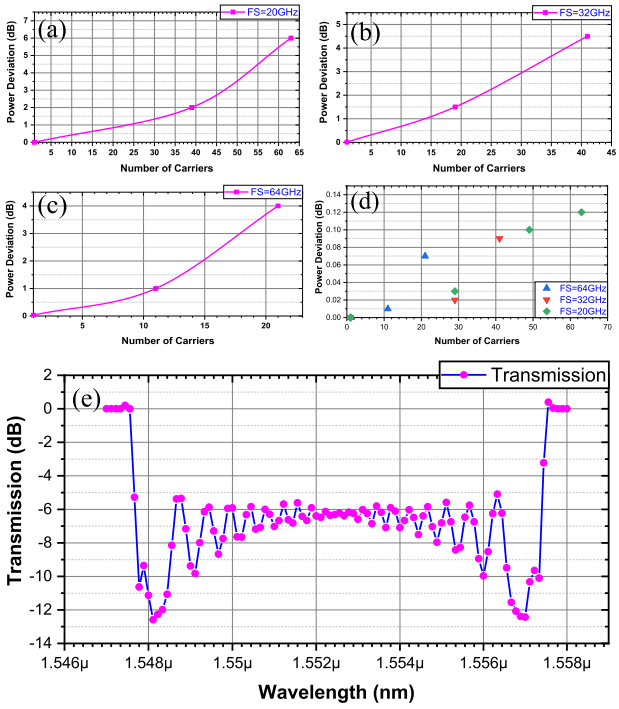

FIGURE 4. Graphical illustration of the PD w.r.t FS. (a) FS = 20GHz, (b) FS = 32GHz, (c) FS = 64GHz. (d) after optimization is performed.

It can be seen in Figure 6 that the RFSV can greatly disturb the number of generated carriers. The maximum number of carriers were generated when the minimum value was considered. A dramatical fall is noticeable in the first two

TABLE 3. Comparison of the proposed work with the cited works.

ref. no	Laser Source	Modulator(s) configuration					Max comb lines (Simulated / Experimental)	FS (GHz)	Approximate Bandwidth (GHz)
		Number of modulators	Single	Parallel	Cascaded	RFS loop			
[1]	EML	2	-	-	☒	-	61	10	~610
[2]	ECL	1	☒	-	-	-	5	19	~95
[6]	DFB	3	-	-	☒	-	29	30	~870
[7]	CW	3	-	-	☒	-	30	61	~1830
[8]	DML	3	-	-	☒	-	78	25	~1950
[9]	ECL	2	-	-	☒	-	15	6	~90
[10]	LD	3	-	-	☒	-	11	40	~480
[11]	CW	2	-	-	☒	-	9	10	~90
[13]	CW	1	☒	-	-	-	256	100MHz	~2.50
[14]	DML	1	☒	-	-	-	16	12.5	~200
[15]	CW	1	☒	-	-	-	~23	18	~468
[16]	CW	3	-	-	☒	-	41	32	~1200
[17]	TLS	3	-	-	-	☒	60	10	~600
[18]	Seed laser	2	-	-	-	☒	80	12.5	~1000
[19]	CW	2	-	-	-	☒	200	12.5	~2.4
[20]	Multiport tunable laser	1	☒	-	-	-	20	10	~190
[21]	DFB	2	-	-	☒	-	20	17	~260
[22]	CW	2	-	☒	-	-	7	25	~170
[23]	CW	1	-	☒	-	-	7	25	~150
[24]	CW	1	-	☒	-	-	9	10	~180
Proposed	CW	2	-	-	☒	-	63	20	~1260

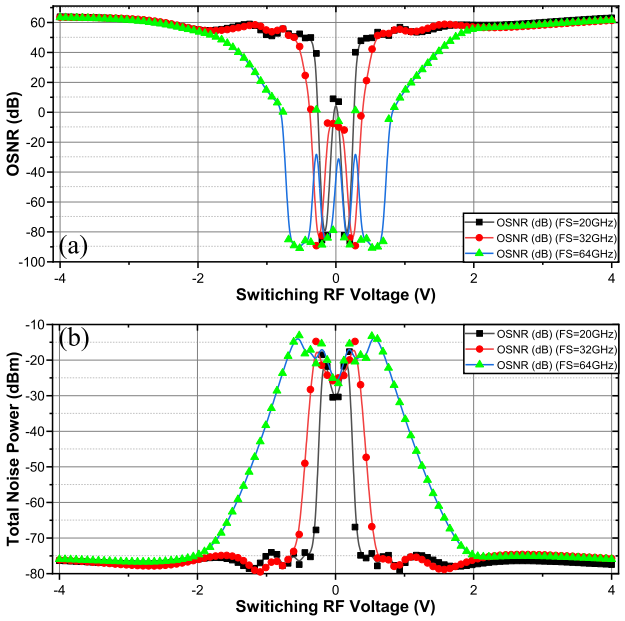

FIGURE 5. Impact of the RFSV on (a) OSNR of the generated spectra, and (b) total noise power.

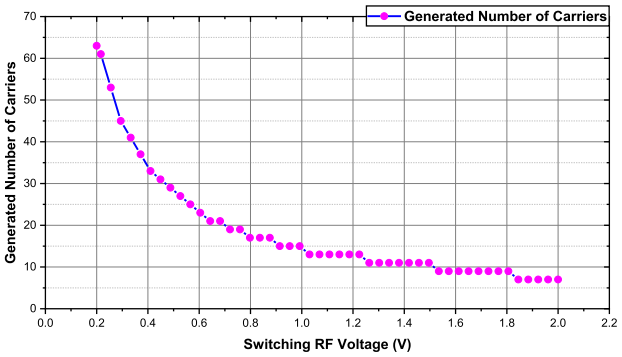

FIGURE 6. RFSV and its impact on the number of generated carriers.

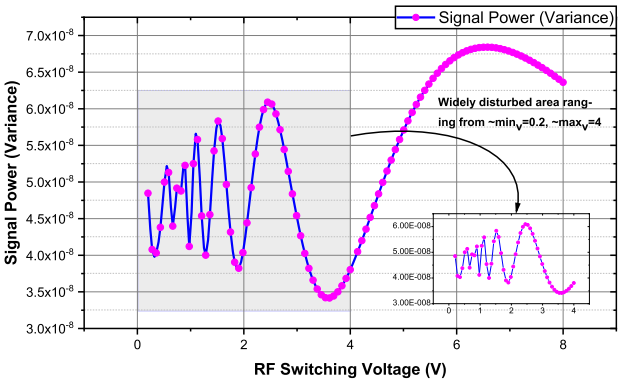

FIGURE 7. RFSV vs signal power (variance).

blocks 0.2-0.6, and the impact is reduced in the latter blocks. It can be noticed that the larger values have less impact on the number of generated carriers. This impact can be studied by the graphical illustration of the RFSV and signal power variance (SPV) in Figure 7.

Figure 7 shows the graphical illustration of the RFSV and SPV when the minimum RFSV value of 0.2V and maximum of 8V is considered. On the other hand, the inset shows the illustration of both SPV and RFSV when the maximum value is limited to 4V. It can be seen that increasing the maximum value results in less variations which greatly influences the

number of generated carriers. Furthermore, an overall comparison of the current scheme is carried out with most of the cited works in Table 3. It is found that the proposed scheme is more efficient in terms of cost efficiency, number of generated carriers, OSNR, TNR, and provides a higher bandwidth. Thus, it can be assumed that the proposed scheme is deployable in coherent optical communications, WDM/OFDM passive optical networks, and advanced modulation based future generation of optical access networks.

IV. CONCLUSION

In this paper, a new cost-proficient and ultra-flattened OFC generation scheme is proposed. In the proposed scheme, cascaded PM and DD-LiNbO$_3$-MZM is utilized to generate the OFC. A total of 63 stable and healthy carriers are achieved with a FS of 20GHz. The proposed scheme is also tested under varying FSs and it is observed that the scheme can handle all the situations comfortably with high TNR and lower PDs. The scheme is analyzed in terms of the PD among the carriers, TNR, OSNR, and number of generated carriers. The simulation results show great performance and, thus, given proper environment, the proposed scheme can be deployed in next generation high-capacity wavelength division multiplexed passive optical networks, and coherent optical communications with advanced modulation techniques.

REFERENCES

[1] R. Ullah, L. Bo, S. Ullah, M. Yaya, F. Tian, and X. Xiangjun, "Cost effective OLT designed from optical frequency comb generator based EML for 1.22 Tbps wavelength division multiplexed passive optical network," *Opt. Fiber Technol.*, vol. 43, pp. 49–56, Jul. 2018, doi: 10.1016/j.yofte.2018.01.025.

[2] J. He, F. Long, R. Deng, J. Shi, M. Dai, and L. Chen, "Flexible multiband OFDM ultra-wideband services based on optical frequency combs," *J. Opt. Commun. Netw.*, vol. 9, no. 5, p. 393, May 2017, doi: 10.1364/JOCN.9.000393.

[3] S. E. Mirnia, A. Zarei, S. D. Emami, S. W. Harun, H. Arof, H. Ahmad, and H. M. H. Shalaby, "Proposal and performance evaluation of an efficient RZ-DQPSK modulation scheme in all-optical OFDM transmission systems," *J. Opt. Commun. Netw.*, vol. 5, no. 9, p. 932, Sep. 2013, doi: 10.1364/JOCN.5.000932.

[4] M. Nakazawa, T. Hirooka, P. Ruan, and P. Guan, "Ultrahigh-speed orthogonal TDM transmission with an optical nyquist pulse train," *Opt. Express*, vol. 20, no. 2, p. 1129, Jan. 2012, doi: 10.1364/OE.20.001129.

[5] B. J. Chun, S. Hyun, S. Kim, S.-W. Kim, and Y.-J. Kim, "Frequency-comb-referenced multi-channel fiber laser for DWDM communication," *Opt. Express*, vol. 21, no. 24, p. 29179, Dec. 2013, doi: 10.1364/oe.21.029179.

[6] C. Chen, C. Zhang, W. Zhang, W. Jin, and K. Qiu, "Scalable and reconfigurable generation of flat optical comb for WDM-based next-generation broadband optical access networks," *Opt. Commun.*, vol. 321, pp. 16–22, Jun. 2014, doi: 10.1016/j.optcom.2014.01.059.

[7] R. Ullah, L. Bo, S. Ullah, M. Yaya, F. Tian, M. K. Khan, and X. Xiangjun, "Flattened optical multicarrier generation technique for optical line terminal side in next generation WDM-PON supporting high data rate transmission," *IEEE Access*, vol. 6, pp. 6183–6193, 2018, doi: 10.1109/ACCESS.2018.2789863.

[8] R. Ullah, S. Ullah, A. Ali, M. Yaya, S. Latif, M. K. Khan, and X. Xin, "Optical 1.56 Tbps coherent 4-QAM transmission across 60 km SSMF employing OFC scheme," *AEU-Int. J. Electron. Commun.*, vol. 105, pp. 78–84, Jun. 2019, doi: 10.1016/j.aeue.2019.04.004.

[9] M. A. Soto, M. Alem, M. A. Shoaie, A. Vedadi, C.-S. Brès, L. Thévenaz, and T. Schneider, "Optical sinc-shaped Nyquist pulses of exceptional quality," *Nature Commun.*, vol. 4, no. 1, p. 2898, Dec. 2013, doi: 10.1038/ncomms3898.

[10] F. Zhang, J. Wu, Y. Li, and J. Lin, "Flat optical frequency comb generation and its application for optical waveform generation," *Opt. Commun.*, vol. 290, pp. 37–42, Mar. 2013, doi: 10.1016/j.optcom.2012.10.051.

[11] X. Zhou, X. Zheng, H. Wen, H. Zhang, Y. Guo, and B. Zhou, "All optical arbitrary waveform generation by optical frequency comb based on cascading intensity modulation," *Opt. Commun.*, vol. 284, no. 15, pp. 3706–3710, Jul. 2011, doi: 10.1016/j.optcom.2011.02.010.

[12] G. Gagliardi, M. Salza, S. Avino, P. Ferraro, and P. De Natale, "Probing the ultimate limit of fiber-optic strain sensing," *Science*, vol. 330, no. 6007, pp. 1081–1084, Nov. 2010, doi: 10.1126/science.1195818.

[13] M. Pelusi, H. N. Tan, K. Solis-Trapala, T. Inoue, and S. Namiki, "Low noise frequency combs for higher order QAM formats through cross-phase modulation of modelocked laser pulses," *IEEE J. Sel. Topics Quantum Electron.*, vol. 24, no. 3, pp. 1–12, May 2018, doi: 10.1109/JSTQE.2017.2769622.

[14] Y. Fukuchi, K. Hirata, and H. Ikeoka, "Wavelength-tunable and bandwidth-variable ultra-flat optical frequency comb block generation from a bismuth-based actively mode-locked fiber laser," *IEEE Photon. J.*, vol. 6, no. 1, pp. 1–9, Feb. 2014, doi: 10.1109/JPHOT.2013.2295469.

[15] W. Jiang, S. Zhao, X. Li, and Q. Tan, "Optical frequency comb generation based on three parallel Mach–Zehnder modulators with recirculating frequency shifting loop," *Opt. Rev.*, vol. 24, no. 4, pp. 533–539, Aug. 2017, doi: 10.1007/s10043-017-0344-9.

[16] J. Li, H. Ma, Z. Li, and X. Zhang, "Optical frequency comb generation based on dual-polarization IQ modulator shared by two polarization-orthogonal recirculating frequency shifting loops," *IEEE Photon. J.*, vol. 9, no. 5, pp. 1–10, Oct. 2017, doi: 10.1109/JPHOT.2017.2745558.

[17] F. Tian, R. Zhang, R. Ullah, B. Wang, Q. Zhang, Q. Tian, B. Liu, Y. Wang, and X. Xin, "Theoretical analysis of high-quality multi-carrier generator based on double complementary re-circulating frequency shifter," *Opt. Commun.*, vol. 445, pp. 222–230, Aug. 2019, doi: 10.1016/j.optcom.2019.03.015.

[18] J. Tang, J. Sun, L. Zhao, T. Chen, T. Huang, and Y. Zhou, "Tunable multiwavelength generation based on Brillouin-Erbium comb fiber laser assisted by multiple four-wave mixing processes," *Opt. Express*, vol. 19, no. 15, p. 14682, Jul. 2011, doi: 10.1364/oe.19.014682.

[19] I. Morohashi, T. Sakamoto, N. Sekine, A. Kasamatsu, and I. Hosako, "Ultrashort optical pulse source using Mach–Zehnder-modulator-based flat comb generator," *Nano Commun. Netw.*, vol. 10, pp. 79–84, Dec. 2016, doi: 10.1016/j.nancom.2016.07.012.

[20] K. Qu, S. Zhao, X. Li, Z. Zhu, D. Liang, and D. Liang, "Ultra-flat and broadband optical frequency comb generator via a single Mach–Zehnder modulator," *IEEE Photon. Technol. Lett.*, vol. 29, no. 2, pp. 255–258, Jan. 15, 2017, doi: 10.1109/LPT.2016.2640276.

[21] S. Preussler, N. Wenzel, and T. Schneider, "Flat, rectangular frequency comb generation with tunable bandwidth and frequency spacing," *Opt. Lett.*, vol. 39, no. 6, p. 1637, Mar. 2014, doi: 10.1364/OL.39.001637.

[22] Q. Wang, L. Huo, Y. Xing, and B. Zhou, "Ultra-flat optical frequency comb generator using a single-driven dual-parallel Mach–Zehnder modulator," *Opt. Lett.*, vol. 39, no. 10, p. 3050, May 2014, doi: 10.1364/OL.39.003050.

[23] J. Yan, S. Zhang, Z. Xia, M. Bai, and Z. Zheng, "A tunable optical frequency comb generator using a single dual parallel Mach–Zehnder modulator," *Opt. Laser Technol.*, vol. 72, pp. 74–78, Sep. 2015, doi: 10.1016/j.optlastec.2015.03.016.

[24] J. Shen, S. Wu, and D. Li, "Ultra-flat optical frequency comb generation based on phase modulation with simple digital driving signal," *Optik*, vol. 198, Dec. 2019, Art. no. 163254, doi: 10.1016/j.ijleo.2019.163254.

[25] X. Li and J. Yu, "W-band RoF transmission based on optical multi-carrier generation by cascading one directly-modulated DFB laser and one phase modulator," *Opt. Commun.*, vol. 345, pp. 80–85, Jun. 2015, doi: 10.1016/j.optcom.2015.01.059.

[26] R. Ullah, L. Bo, S. Ullah, M. Yaya, F. Tian, and X. Xiangjun, "Proposing simulation model for multi-wavelength source offering 40 Gbps WDM-PON using AWG with a single laser," *Comput. Appl. Eng. Edu.*, vol. 27, no. 6, pp. 1299–1307, Nov. 2019, doi: 10.1002/cae.22085.

[27] X. Lv, J. Liu, and S. Wu, "Flat optical frequency comb generation based on polarization modulator with RF frequency multiplication circuit and dual-parallel mach-zehnder modulator," *Optik*, vol. 183, pp. 706–712, Apr. 2019, doi: 10.1016/j.ijleo.2019.02.114.

[28] R. Ullah, L. Bo, M. Yaya, F. Tian, A. Ali, I. Ahmad, M. S. Khan, and X. Xiangjun, "Application of optical frequency comb generation with controlled delay circuit for managing the high capacity network system," *AEU-Int. J. Electron. Commun.*, vol. 94, pp. 322–331, Sep. 2018, doi: 10.1016/j.aeue.2018.07.025.

[29] S. Ullah, B. Liu, R. Ullah, M. Ahmad, F. Wang, L. Zhang, X. Xin, K. A. Memon, and H. A. Khalid, "Generation of flattened multicarrier signals from a single laser source for 330 Gbps WDM-PON transmission over 25 km SSMF," *J. Opt. Commun.*, vol. 39, no. 1, Dec. 2017, doi: 10.1515/joc-2017-0183.

[30] S. Ullah, R. Ullah, A. Khan, H. A. Khalid, Q. Zhang, Q. Tian, F. Khan, and X. Xin, "Optical multi-wavelength source for single feeder fiber using suppressed carrier in high capacity LR-WDM-PON," *IEEE Access*, vol. 6, pp. 70674–70684, 2018, doi: 10.1109/ACCESS.2018.2880426.

[31] J. Zhang, N. Chi, J. Yu, Y. Shao, J. Zhu, B. Huang, and L. Tao, "Generation of coherent and frequency-lock multi-carriers using cascaded phase modulators and recirculating frequency shifter for Tb/s optical communication," *Opt. Express*, vol. 19, no. 14, p. 12891, Jul. 2011, doi: 10.1364/oe.19.012891.

SIBGHAT ULLAH received the B.S.C.S. degree from the University of Peshawar, and the master's degree in electronics and communication engineering from the Beijing University of Posts and Telecommunications, Beijing, China, where he is currently pursuing the Ph.D. degree with the State key Laboratory of Information Photonics and Optical Communications. His research interests include coherent optical communications, optical multicarrier/frequency comb generation, wavelength division multiplexed passive optical networks, and long reach PON.

RAHAT ULLAH received the M.Sc. degree in electronics from the University of Peshawar, Pakistan, in 2008, and the M.S. (CS) degree in telecommunication and networking from Gandhara University, Peshawar, Pakistan, in 2012, and the Ph.D. degree in optical engineering from the Beijing University of Posts and Telecommunications and honored with the outstanding Ph.D. student award of 2017. He worked as a Lecturer/Assistant Professor with Sarhad University, Peshawar, for six years. He is currently working as an Asscoaite Professor with the Institute of Optoelectronics, Nanjing University of Information Science and Technology, China. His research interests include optical communications, passive optical networks, optical multicarriers generation, and radio over fiber.

QI ZHANG received the Ph.D. degree from BUPT, Beijing, China, in 2005, where she is currently an Associate Professor with the School of Electric Engineering and a member of the State Key Laboratory of Information Photonics and Optical Communications. Her main research interests focus on optical communication and satellite communication.

HAFIZ AHMAD KHALID received the B.S. degree in electronics engineering from the COMSATS Institute of Information Technology, Abbottabad, Pakistan, in 2010, and the M.S. degree in electrical engineering from the University of Engineering and Technology, Taxila, Pakistan, in 2015. He is currently pursuing the Ph.D. degree in electronics science and technology with the Beijing University of Posts and Telecommunications, Beijing, China. From 2013 to 2016, he was a Lecturer with the Wah Engineering College, University of Wah, Wah Cantt, Pakistan. His research interest includes the wireless and optical MIMO communication.

KAMRAN ALI MEMON (Member, IEEE) received the bachelor's degree in electronics from the Mehran University of Engineering Technology, Jamshoro, Pakistan, in 2009, and the master's degree in communication from Quaid e Awam UEST Nawabshah, Pakistan, in 2015. He is currently pursuing the Ph.D. degree with the State Key Laboratory of Information Photonics and Optical Communications (IPOC), Beijing University of Posts and Telecommunications, China. He worked as a Lecturer/Assistant Professor with QUEST, Pakistan, for seven years. He is the author of several research articles published in journals of world class repute. His research interests include optical and wireless communications, DBA schemes in PONs, ROF, and WSNs.

ADIL KHAN received the B.S. degree in telecommunications from Iqra National University, Peshawar, and the master's degree in electronics and communication engineering from the Beijing University of Posts and Telecommunications, Beijing, China, where he is currently pursuing the Ph.D. degree. His research interests include wireless communication, full duplex communication in 5G, and antenna design.

FENG TIAN was born in Shangdong, China. She received the B.S. degree in communication engineering from the Chongqing University of posts and Telecommunication, Chongqing, China, in 2008, and the Ph.D. degree in physical electronics from the Beijing University of Posts and Telecommunication, Beijing, China, in 2013. She is currently working as an Assistant Professor with the School of Electronics Engineering, Beijing University of Posts and Telecommunications. She has authored and coauthored more than 40 international journals and peer-reviewed conference papers. Her research focuses on high-speed fiber communication systems, including multicarrier generation, PMD compensation in fibers, multilevel phase modulation formats, and recovery of optical signal distortions.

XIN XIANGJUN was born in Hebei, China, in 1969. He received the Ph.D. degree from the School of Electric Engineering, Beijing University of Posts and Telecommunications (BUPT), Beijing, China, in 2004. He is currently a Professor with the School of Electric Engineering and a member of the State Key Laboratory of Information Photonics and Optical Communications, BUPT. His main research interests focus on broadband optical transmission technologies, optical sensor, and all-optical networks. Within this area, he has published more than 60 SCI articles.